

LES of Turbulent Mixing In Anti-Vortex Film Cooling Flows

Abdel-Mohimen^a and Higazy^a

^aDepartment of Mechanical Engineering, Benha University, Faculty of Engineering, 108 shoubra street, Cairo, Egypt.

Accepted 01 November 2013, Available online 01 December 2013, (Nov/Dec 2013 issue)

Abstract

The Anti-vortex film cooling technique is investigated by using large eddy simulation (LES) due to its complex mixture between the mainstream flow, the film cooling flow, and the flow through the anti-vortex holes. A geometry of single row of 30 degree round holes on a flat plate is used as the baseline case. Three different values of velocity ratios (Coolant Jet Velocity/Main Stream Velocity) are studied. Two different positions of the anti-vortex holes are investigated with temperature ratio (main stream temperature / coolant temperature) namely 2. The density ratio is taken in consideration. Use of symmetry boundary condition is avoided to capture three dimensional, unsteady, turbulent nature of the flow. Present simulation is carried out by using FLUENT commercial code. Numerical calculation of film cooling effectiveness is validated with reported experimental results. Results show that the used anti-vortex technique improves the film cooling effectiveness. The numerical boundary layer velocity vectors showed that the anti-vortex holes create reverse vortices against the main vortices that are created by the main hole. These reverse vortices help in keeping the coolant jet flow near the surface.

Keywords: Anti-Vortex, film cooling, turbine blade cooling.

1. Introduction

Film Cooling is the introduction of a secondary fluid (coolant or injected fluid) at one or more discrete locations along a surface exposed to a high temperature environment to protect that surface not only in the immediate region of injection but also in the downstream region [8]. Flat surface film cooling has been known and subjected to research for a long time. Goldstein et al. [9] described the effectiveness characteristics with lateral injection. The effectiveness following single hole of the inclination angle of 15 and 35 deg were investigated. They reported that the effect of lateral injection is to widen the temperature field and decrease the peak effectiveness for the blowing ratio of $BR=0.5$. For the higher blowing ratios, however, the lateral injection increases both the width of the temperature field and the peak film cooling effectiveness. Ammari et al. [1] also presented the effect of density ratio on heat transfer coefficient contours downstream of a film hole inclined 35° along the stream-wise direction for two different coolant-to-mainstream density ratios of 1.0 and 1.52 for a coolant blowing ratio of $BR=1.46$. Differences of 10% in film cooling occurred when coolant densities were changed. Andreopoulos and Rodi [2] studied the behavior of a single jet and mainstream interaction. There is a mutual deflection of

the jet and the mainstream. The jet is pushed towards the bottom wall and the mainstream is deflected as if the jet forms a solid boundary. At a low momentum ratio $MR=0.25$, the mainstream pushes the jet to adhere to the bottom wall. At a higher momentum ratio $MR=4.0$, the jet penetrates into the mainstream before it is bent. Alok Dhungel [5] investigated the enhanced cooling performance caused by addition of anti-vortex holes to the main cylindrical film cooling holes. Both heat transfer coefficient and film cooling effectiveness are determined experimentally downstream of the exit of the film cooling holes on a flat plate by a single test using the transient Infra Red thermography technique. A total of six different cases with variations in geometry and orientation of the anti-vortex holes in relation to the main film cooling holes are thoroughly investigated. Results suggested that the presence of anti-vortex holes mitigates the effect of the pair of anti vortices. Heidmann [11] and Heidmann et al [12] used a 3-D Navier-Stokes solver Glenn-HT which has been conceived and developed at NASA Glenn Research Center to study the "anti-vortex" film-cooling concept which is designed to mitigate the effects of the counter-rotating vortex pair, which reduces the effectiveness of circular cross-section film-cooling holes at moderate to high blowing ratios. Preliminary and improved designs concepts are developed in this study, although many

parameters can be modified in an optimized design. The concept is applied in this study as a modification to a standard single row round film-cooling hole arrangement with the holes angled at 30 deg to the surface and a span-wise pitch of three hole diameters and is compared to the base line data of Dhungel et al [6]. The present work use the LES model to investigate and show the interaction between the flow through the main film cooling hole and the main stream in the presence of the flow through the anti-vortex holes. Also the enhancement in the film cooling effectiveness due to the use of anti-vortex technique is presented and discussed.

1.1 Studied Geometries

Figure (1) describes schematic control volume of mainstream air passing over an adiabatic flat surface (e.g., a turbine blade). The surface of study has a row of injection cylindrical holes through which coolant air is passed into the mainstream at 30o inclined angle with the horizontal. The temperature ratio (main stream temperature / coolant temperature) is namely 2. That means the hot air is coming out from the coolant jet holes while the mainstream air is the cooling one. This technique is applied to easy compare with an experimental work use the same technique [13]. Using of coolant jet with lower temperature than the mainstream flow is tested and it gives the same results as compared with the used technique. A fixed free stream mean velocity of 8.6 m/s is applied while different velocity ratios are achieved by changing the coolant jets mass flow rate. The velocity ratio (VR) is the ratio of the injectant mean velocity to free-stream mean velocity. The velocity ratio values are 0.5, 1.0, and 2.0.

Baseline case is a flat surface with three inclined holes. The diameter of each hole is 10 mm and the spacing between the holes is 3D. The length of holes is 4D. The holes are inclined to the horizontal at an angle of 30o along the flow direction. A pair of anti-vortex holes were added each to all the three film cooling holes. The orientations and other geometries of the primary film cooling hole is the same as the baseline, only the features of the anti-vortex film cooling holes are altered.

Two different geometries are investigated. The details of the geometry are presented in figure (2) where the distance between the center of the anti-vortex holes and the center of the primary film cooling holes measured in the x- direction is represented by parameter 'a'. The similar distance measured in the y- direction is given by parameter 'b'. The angle measured in degrees between the axis of the primary film cooling holes and the anti-vortex holes measured in the front vertical plane is represented by parameter 'R'. Similar angle measured in the side vertical plane is represented by parameter 'Q'. Parameter 'D' and 'd' represents the diameters of the primary film cooling holes and the anti-vortex holes

respectively. Table (1) shows the values of D, d, a, b, R, Q for studied cases.

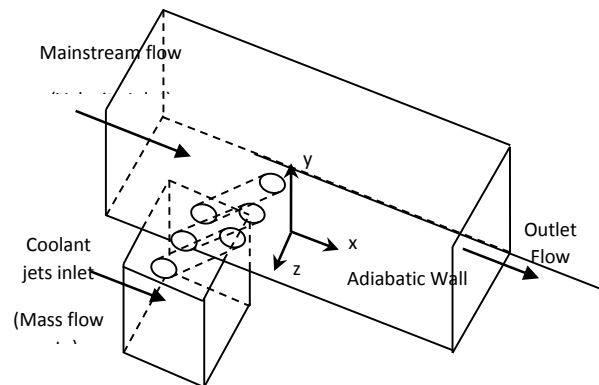


Fig.1. Schematic of the film cooling flow and boundary conditions

Case-1: as shown in figure 3 (a), the anti-vortex holes shoot out vertically upwards from the primary film cooling holes and thus the exit of the anti-vortex holes is far upstream as compared to the exit of the primary film cooling hole. The anti-vortex hole originate from the lower end of the primary film cooling hole

Case-2: as shown in fig. 3 (b), the exit of the anti-vortex film cooling holes are still upstream to the outlet of the primary film cooling hole but isn't far as compared to case-1. Both the anti-vortex film cooling holes are symmetrical in orientation and location to the primary film cooling hole.

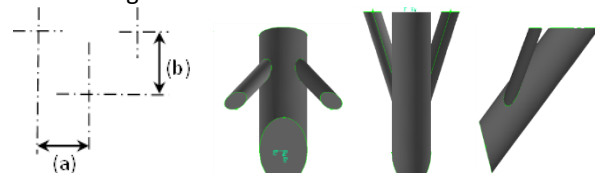


Fig.2. Anti-Vortex Hole Configuration

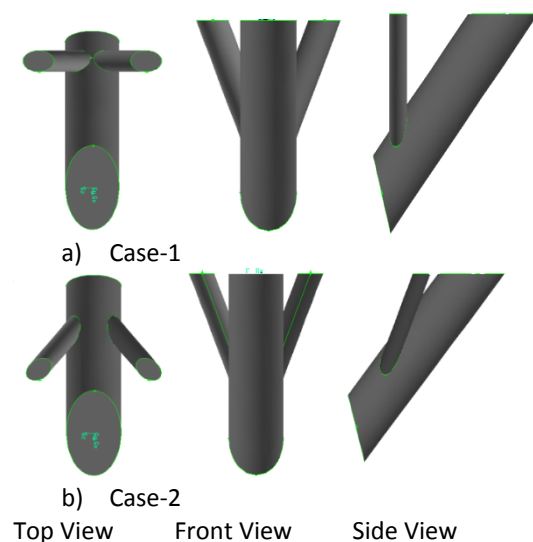


Fig.3. Anti-Vortex Hole Orientations

Table 1 Test Plate Details (DEPENDING ON FIG. 2)

	Case 1	Case 2
D	10	10
d	5	5
a	10	10
b	30	15
Q	90	49.1
R	30	30

(Dimensions in mm and angles in degrees)

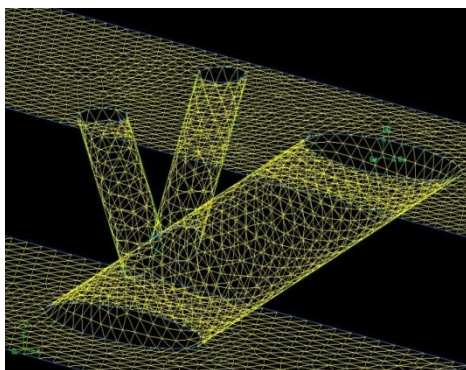
2. Numerical Method

Supporting the three-dimensional flow CFD studies are performed to gain a deeper insight into the flow field that is responsible for the observed coolant jet interaction with the mainstream. FLUENT is used to simulate film cooling for all anti-vortex geometries and compared to baseline case cylindrical holes. The computational grid is shown in Figure (4). The Figure highlights the grid quality near the hole intersection region for case (1). Mainstream conditions were maintained the same in all cases and the coolant flow rate was altered to change the velocity ratios. At solid walls, adiabatic boundary conditions are used, and no-slip boundary condition is set as:

$$U_w = 0, V_w = 0, W_w = 0, \overline{u_i' u_j'} = 0$$

where index w denotes the wall.

For the mainstream and the coolant jet velocity inlet, uniform profile is set. In our study, all the computations are performed with uniform flow inlet for the mainstream and the coolant jet. Standard total temperature value and inlet velocity were used at the mainstream inlet with flow normal to the inlet plane. The mainstream inlet is 20 D upstream of the main hole center line. The plenum inlet mass flow rate was adjusted to produce the blowing ratio desired. The plenum inlet total temperature was set to 2 times the mainstream inlet total temperature.

**Fig.4.** Hole Intersection Grid Close-Up

FLUENT is based on an unstructured grid solver using a finite volume approach for the solution of the Reynolds Averaged Navier-Stokes (RANS) equations. An

unstructured computational grid was developed using the Gambit grid generator with approximately 1.5 million computational cells for each case. All the cases presented here converged to residual levels of the order of 10^{-7} for velocity components and energy equation and 10^{-5} for mass flow rate. An investigation of grid independence was carried out to find the proper mesh. The test was performed on the baseline.

2.1 Turbulence Model

The complex dynamic nature of the film cooling flow makes it necessary to model the vortices using temporally and spatially accurate calculation of the flow field to capture the dominant turbulence length scales. Turbulent flows are characterized by eddies with a wide range of length and time scales. The largest eddies are typically comparable in size to the characteristic length of the mean flow. The smallest scales are responsible for the dissipation of turbulence kinetic energy. It is theoretically possible to directly resolve the whole spectrum of turbulent scales using an approach known as direct numerical simulation (DNS). DNS is not, however, feasible for practical engineering problems.

Large Eddy Simulation (LES) provides an alternative approach in which the large eddies are computed in a time dependent simulation that uses a set of "filtered" equations. Filtering is essentially a manipulation of the exact Navier-Stokes equations to remove only the eddies that are smaller than the size of the filter, which is usually taken as the mesh size.

Filtering the incompressible Navier-Stokes equations, one obtains

$$\text{and } \frac{\partial \rho}{\partial t} + \frac{\partial}{\partial x_i}(\rho \bar{u}_i) = 0$$

$$\frac{\partial}{\partial t}(\rho \bar{u}_i) + \frac{\partial}{\partial x_j}(\rho \bar{u}_i \bar{u}_j) = \frac{\partial}{\partial x_j} \left(\mu \frac{\partial \bar{u}_i}{\partial x_j} \right) - \frac{\partial \bar{p}}{\partial x_i} - \frac{\partial \tau_{ij}}{\partial x_j}$$

Where τ_{ij} is the subgrid-scale stress defined by

$$\tau_{ij} \equiv \rho \bar{u_i' u_j'} - \rho \bar{u}_i \bar{u}_j$$

The subgrid-scale stresses resulting from the filtering operation are unknown, and require modeling. The majority of subgrid-scale models in use today are eddy viscosity models of the following form:

$$\tau_{ij} - \frac{1}{3} \tau_{kk} \delta_{ij} = -2\mu_t \bar{S}_{ij}$$

where μ_t is the subgrid-scale turbulent viscosity, and S_{ij} is the rate-of-strain tensor for the resolved scale defined by

$$\bar{S}_{ij} \equiv \frac{1}{2} \left(\frac{\partial \bar{u}_i}{\partial x_j} + \frac{\partial \bar{u}_j}{\partial x_i} \right)$$

The effectiveness calculation are made with the mainstream at temperature equal to 30 oC, the coolant air heated, and is assumed to be adiabatic. The film

cooling effectiveness is calculated by using equation (6). Since the test surface is adiabatic, there is no heat transfer at the surface. As a result, the local film temperature, T_f , is equal to the corresponding adiabatic wall temperature, T_{aw} . Now the following equation can be used to calculate the film cooling effectiveness.

$$\eta = \frac{T_{aw} - T_m}{T_c - T_m}$$

This method of calculating of the film effectiveness has been used by several researches such as Ou et al. [19] and Mehendale and Han [18].

3. Results and Discussions

Figures (5), (6), and (7) show a comparison between the boundary layer velocity distributions colored by effectiveness for baseline case, case-1, and case-2 at different values of velocity ratios. The boundary layer velocity distribution will be presented in $y - z$ plan from $z/D = -1.5$ to $z/D = 1.5$ at $x/D = 4$ due to clear details of the interaction between the mainstream flow and the coolant jets.

For Baseline case, Figure (5) shows two vortices due to the interaction between the mainstream flow and the jet flow. As the velocity ratio increases, the two vortices lift off the coolant jet away from the test surface due to high momentum flux.

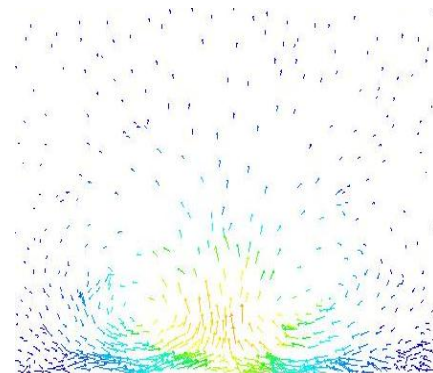
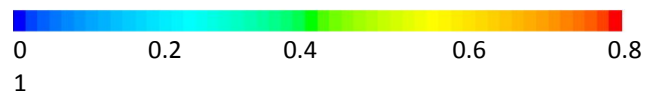
For Case 1, figure (7) shows that there are new vortices, from the anti-vortex holes, appears above the two vortices coming out from the main hole. The new vortices try to move against the main hole vortices keeping the coolant flow near the test surface. This action is very clear with high velocity ratios but it is not clear with low velocity ratios because the fluid flow through the anti-vortex holes is taken from the main hole fluid and for low velocity ratios, the main hole flow is already low. Case 2 has the same performance like case 1. Vortices coming out from the anti-vortex holes try to damping the vortices coming out from the main hole, because the anti-vortex holes are still upstream the main hole

Fig. 7 shows the effect of velocity ratio on detailed film cooling effectiveness distributions for all studied cases. For the baseline case, It is clear that the highest film cooling effectiveness occurring with the lowest velocity ratio ($VR = 0.5$). As the velocity ratio increases, there is a jet lift-off causing lower effectiveness.

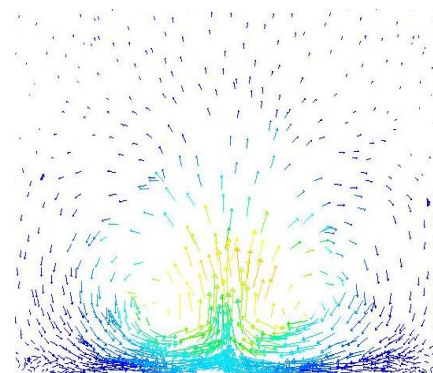
For case 1, the effectiveness is higher than baseline case for all velocity ratios but the trend is different, as the velocity ratio increases the film effectiveness increases and covers bigger area. The anti-vortex pair cause reduced flow through the main hole and also supplements the overall coverage in the region between the holes. It appears that the anti-vortex holes produce a small vortex pair counter to the main vortex pair. It is clearly visible that the highest effectiveness occurs at velocity ratio of 2.0. The effect of this anti-vortex pair

appears to mainly reduce the coolant momentum flux from the main holes.

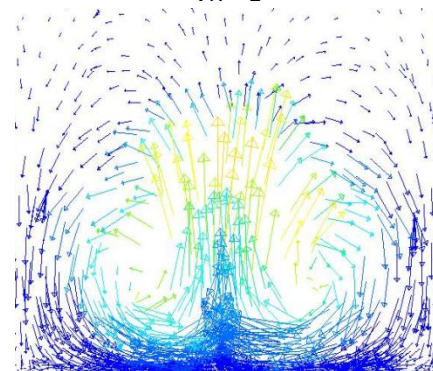
For case 2, the anti-vortex holes are still exit upstream of the main hole but more close to the main hole than in case 1. Like in case 1, the film effectiveness increases as the velocity ratio increases.



VR = 0.5

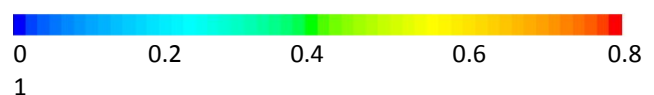


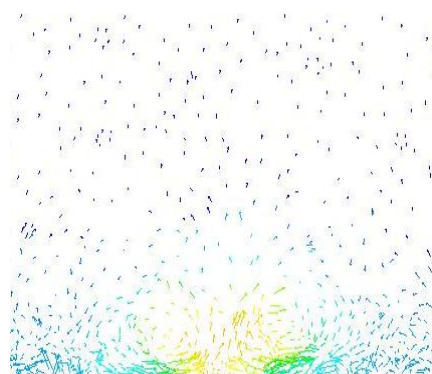
VR = 1



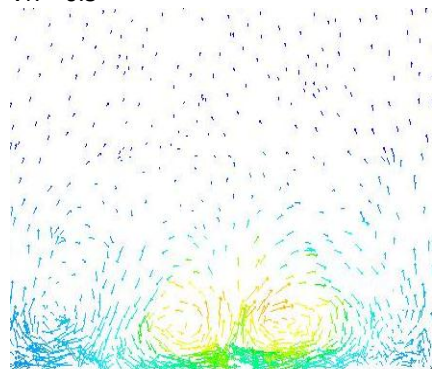
VR = 2

Fig. 5 Secondary flow vectors colored by Effectiveness for Baseline Case at different values of VR, $x/D = 4$

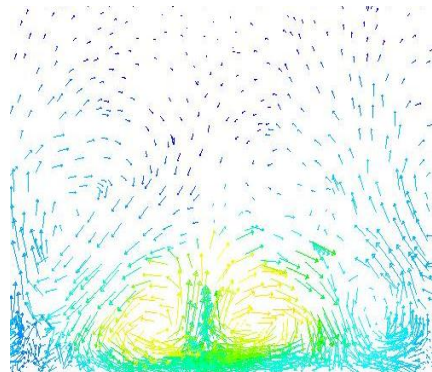




VR = 0.5

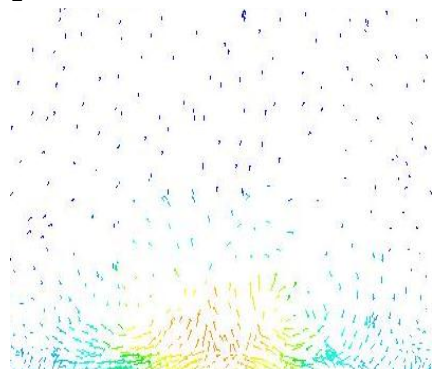


VR = 1

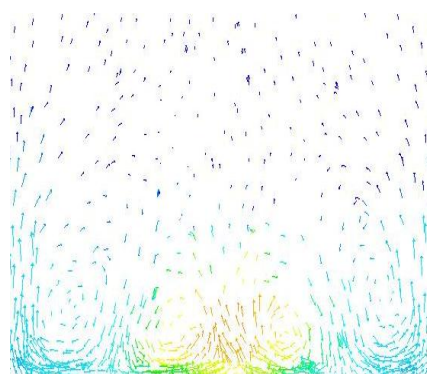


VR = 2

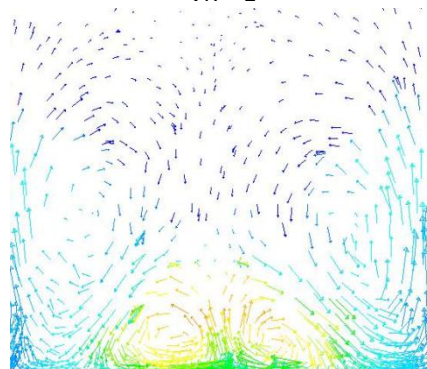
Fig. 6 Secondary flow vectors colored by Effectiveness for Case-1 at different values of VR, $x/D = 4$



VR = 0.5

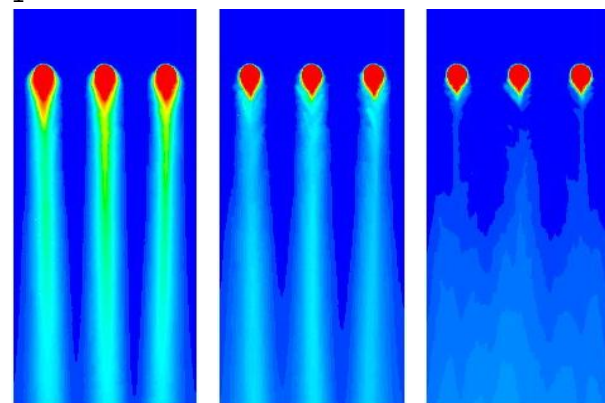
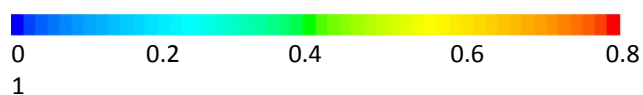


VR = 1

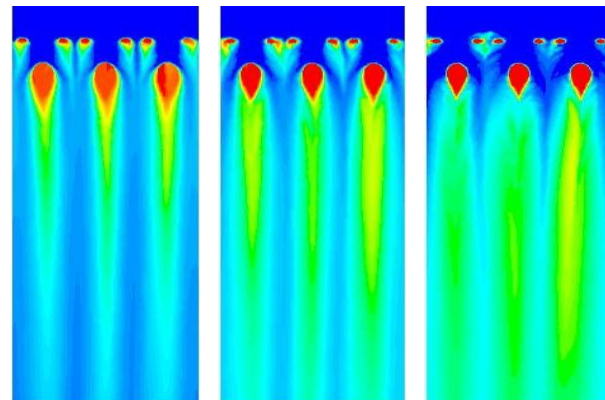


VR = 2

Fig. 7 Secondary flow vectors colored by Effectiveness for Case-2 at different values of VR, $x/D = 4$



Baseline Case



Case 1

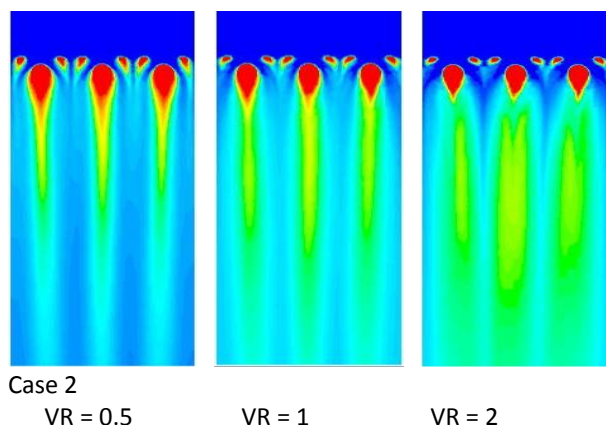


Fig. 8 Detailed Film Cooling Effectiveness Distributions for Studied Cases at different Velocity ratios

The spanwise averaged is calculated for points from $z/D = 1.5$ to $z/D = -1.5$, it means that the spanwise averaged film cooling effectiveness will be presented downstream the middle hole.

For $VR = 0.5$, Fig. (9) shows that, for all cases the spanwise film effectiveness decreases as x/D increases. The momentum ratio at $VR = 0.5$ is low and accordingly the jet flow doesn't penetrate the main stream flow. It moves below the main stream flow and the film cooling effectiveness continuous to decrease with x/D for all cases. The anti-vortex cases give a higher film cooling effectiveness as compared with baseline case. The film cooling effectiveness with anti-vortex cases appears close to each other. Such improvement in film cooling effectiveness can be explained by the close contact between the cooling fluid and the surface. For $VR = 1.0$, Fig. (10) shows that, baseline case has a different trend as compared to other cases. For baseline case, the film effectiveness starts from high value near the hole exit and begins to decrease rapidly until $x/D = 5$ then the film effectiveness begins to increase slowly. Case 1 and case 2 have the same trend (as the coolant fluid is moving downstream the film holes, the film effectiveness decreases gradually). For $VR = 2.0$, Fig. (11) shows that the highest spanwise averaged film cooling effectiveness is given by case 2. For both case 1 and case 2, the film effectiveness may be assumed to be constant along the studied area.

Figure (12) shows the overall area averaged film cooling effectiveness for all studied cases at different values of velocity ratios. The overall area averaged film cooling effectiveness is calculated for the area downstream the middle hole only. The overall area at which the averaged film cooling is calculated is ranged from $x/D = 0$ to $x/D = 26$, and $z/D = -1.5$ to $z/D = 1.5$ for $y/D = 0$. The figure shows that:

For baseline case, as the velocity ratio increases, the overall film effectiveness decreases. For case 1, as the velocity ratio increases, the overall film effectiveness

increases. Case 2 gives the highest overall effectiveness at $VR = 2.0$.

From the above results, for baseline case, the momentum ratio increases with high velocity ratios, so the coolant jet has the ability to penetrate the mainstream flow. According to that, at high velocity ratios, the film cooling effectiveness starts from high value at the film cooling hole and suddenly decreases as moving away from the film cooling hole then starts to increase gradually as the jet flow mixes with the mainstream flow. For anti-vortex cases, the jet flow distributes through the main hole and the anti-vortex holes. In cases 1 and 2, the flow from the anti-vortex holes is moving above the flow from the main hole and is trying to mitigate it to move beside the test surface.

Figures (13) shows a comparison between the present work and previous works at $VR = 2.0$ for baseline case. Dhungel [5] baseline result was taken for $\frac{1}{2}$ inch main hole diameter with angle of inclination equal 30° . Dhungel used infrared camera to measure the temperature distribution on the test surface. Jung et. al. [13] studied the effect of orientation angle. Their baseline was a hole with 35° inclination angle and 20 mm diameter. They used liquid crystal technique to measure the temperature distribution. Figure shows an agreement between the present results with experimental results of Dhungel [5] and Jung et al.[13].

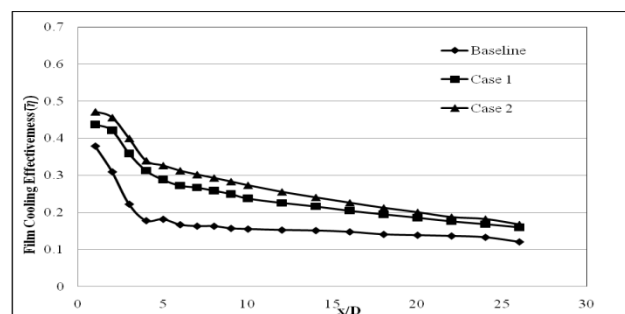


Fig. 9 Effect of Anti-vortex Hole Geometry on Spanwise Averaged Film Cooling Effectiveness Distributions at $VR = 0.5$

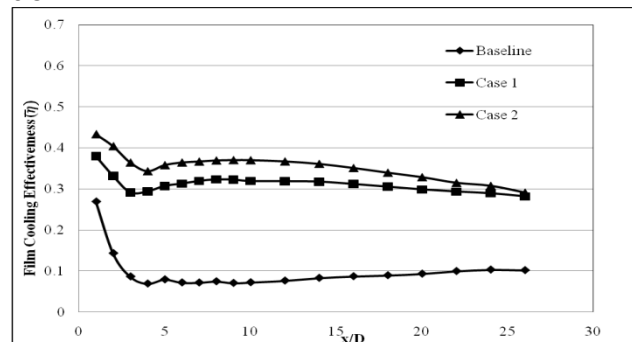


Fig. 10 Effect of Anti-vortex Hole Geometry on Spanwise Averaged Film Cooling Effectiveness Distributions at $VR = 1.0$

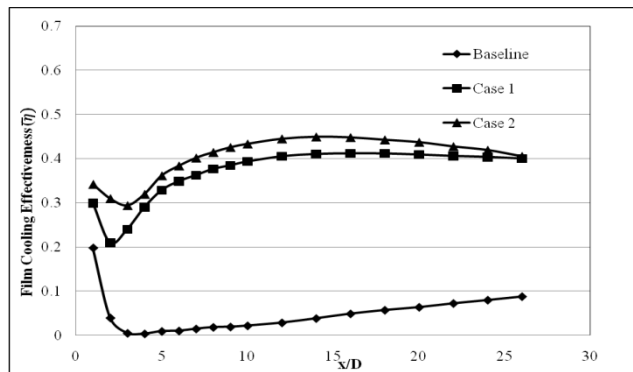


Fig. 11 Effect of Anti-vortex Hole Geometry on Spanwise Averaged Film Cooling Effectiveness Distributions at VR = 2.0

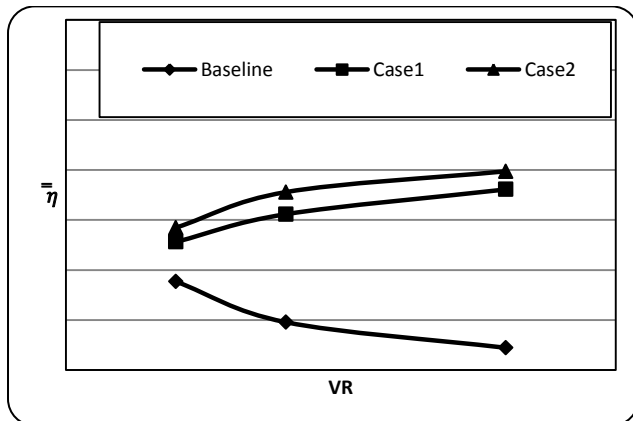


Fig. 12 The overall averaged area film cooling effectiveness for all studied cases with different VR

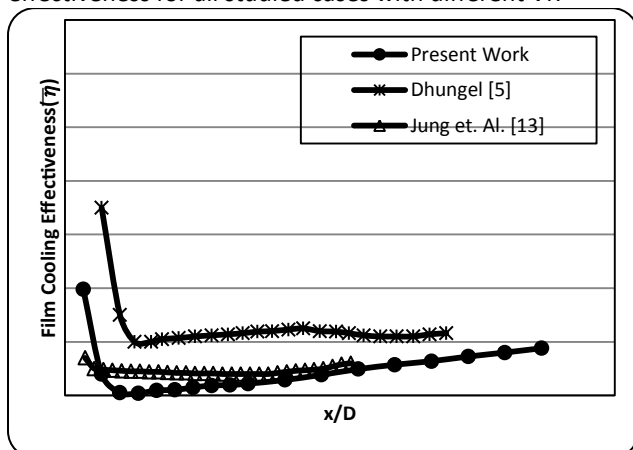


Fig. 13 Comparison of Spanwise averaged film cooling effectiveness distribution for baseline case, VR = 2.0

4. Conclusions

A Computational model is constructed to study numerically, by using the LES model, the effect of using anti-vortex holes branching out from the main film cooling holes on the film cooling effectiveness. Different values of velocity ratios VR, (coolant jet velocity/main

stream velocity) namely 0.5, 1.0, and 2.0, are studied with two different positions of anti-vortex holes. The following points represent the main conclusions.

1. Results show that the use of anti-vortex holes enhance the film cooling downstream the film cooling holes. It appears that the presence of anti-vortex holes mitigates the effect of the kidney vortices and also reduces the momentum of the main jet hence improving the film coverage in both downstream and lateral direction.
2. For baseline case, as the velocity ratio increases, the overall area-averaged film cooling effectiveness decreases. On the contrary, for all cases with anti-vortex as the velocity ratio increases, the overall area averaged film cooling effectiveness increases.
3. The overall area averaged film cooling effectiveness generally increases with the use of anti-vortex.
4. The use of LES gives a good agreement with experimental results and help in catching the intersection behavior between the mainstream flow and the film cooling jets.

References

- [1] Ammari, H.D., Hay, N., and Lampard, D., 1990 "The Effect of Density Ratio on the Heat Transfer Coefficient from a Film Cooled Flat Plate." ASME Journal of Turbomachinery, Vol. 112, pp444-450.
- [2] Andreopoulos, J. and Rodi, W., 1984 "Experimental Investigation of Jets in Crossflow" Journal of Fluid Mechanics, Vol 138, pp 93-127
- [3] Bons, J.P., MacArthur, C.D., and Rivir, R.B., 1996, "The Effect of High Free-Stream Turbulence on Film Cooling Effectiveness." ASME Journal of Turbomachinery, Vol.118, pp.814-825.
- [4] Bunker, R. S., 2005, "A Review of Shaped Hole Turbine Film-Cooling Technology," ASME J. Heat Transfer, 127, pp. 441-453.
- [5] Dhungel, A., 2007, "Film Cooling from a Row of Holes Supplemented with Anti-vortex Holes" A Thesis for the degree of Master of Science in Mechanical Engineering, Louisiana State University.
- [6] Dhungel, S., Phillips, A., Ekkad, S. V., and Heidmann, J. D., 2007, "Experimental Investigation of a Novel Anti-Vortex Film Cooling Hole Design," ASME Paper No. GT2007-27419.
- [7] FLUENT Guide Book
- [8] Foster, N.W., Lampard, D., "The Flow and Film Cooling Effectiveness Following Injection Through a Row of Holes", ASME Journal of Eng. Power 102 (1980) pp. 584-588
- [9] Goldstein, R. J., Eckert, E. R. G., Eriksen, V. L., and Ramsey, J. W., 1970, "Film Cooling Following Injection Through Inclined Circular Tubes," Israel Journal of Technology, Vol. 8, No. 1-2, pp. 145-154.
- [10] Haven, B. A., Yamagata, D. K., Kurosaka, M., Yamawaki, S., and Maya, T., 1997, "Anti-Kidney Pair of Vortices in Shaped Holes and Their Influence on Film Cooling Effectiveness," ASME Paper No. 97-GT-45.
- [11] Heidmann, J. D., 2008, "A Numerical Study of Anti-Vortex Film Cooling Designs at High Blowing Ratio" NASA/TM-2008-215209.
- [12] Heidmann, J. D., Ekkad, S., 2008, "A Novel Antivortex Turbine Film-Cooling Hole Concept" Journal of Turbomachinery, ASME, JULY 2008, Vol. 130.
- [13] Jung, I. S., and Lee J. S., 2000, "Effects of Orientation Angles on Film Cooling Over a Flat Plate: Boundary Layer Temperature Distributions and Adiabatic Film Cooling Effectiveness" Journal of Turbomachinery, ASME, Jan 2000, Vol.122, pp 153 - 160.
- [14] Kline, S.J. and McClintock, F.A., 1953, "Describing Uncertainties in Single Sample Experiments," Mechanical Engineering, Vol. 75, pp. 3-8.
- [15] Kohli, A., Bogard, D., "Adiabatic Effectiveness Thermal fields and Velocity Fields for Film Cooling with Large Angle Injection", ASME Journal of Turbomachinery, 119(1997) pp.352-358.
- [16] Lemmon, C. A., Kohli, A., and Thole, K. A., 1999, "Formation of Counter-Rotating Vortices in Film-Cooling Flows," ASME Paper No. 99-GT-161.
- [17] Leylek, J.H., and Zerkle, R.D., 1994. "Discrete-jet Film Cooling: A Comparison of Computational Results with Experiments" ASME Journal of Turbomachinery, Vol. 116, pp358-368.
- [18] Mehendale, A.B., and Han, J.C., 1992, "Influence of High Mainstream Turbulence on Leading Edge Film Cooling Heat Transfer: Effect of Film Hole Spacing" Int. J. of Heat Mass Transfer, 35, No. 10, pp. 2593-2604.
- [19] Ou, S., Han, J.C., Mehendale, A.B., and Lee, C.P., 1994, "Unsteady Wake Over a Linear Turbine Blade Cascade with Air and CO2 Film Injection. Part I: Effect on Heat Transfer Coefficients", ASME J. Turbomachinery, 116, pp. 721-729.
- [20] Yiping Lu, "Effect of Hole Configurations on Film Cooling from Cylindrical Inclined Holes for The Application to Gas Turbine Blades", partial fulfillment of the requirements for the degree of Doctor of Philosophy, Louisiana State University, December 2007.